DOI:10.5277/ABB-00366-2015-03

Computational analysis of aortic hemodynamics during total and partial extra-corporeal membrane oxygenation and intra-aortic balloon pump support

Maria Vittoria Caruso[1*], Vera Gramigna[1], Attilio Renzulli[2], Gionata Fragomeni[1]

[1]Bioengineering Group, Department of Medical and Surgical Sciences, Magna Graecia University, Catanzaro, Italy

[2]Cardiothoracic Surgery, Department of Medical and Surgical Sciences, Magna Graecia University, Catanzaro, Italy

*Corresponding Author:

Maria Vittoria Caruso, Bioengineering Group, Department of Medical and Surgical Sciences, Magna Graecia University, Catanzaro, Italy. Tel: +39 09613694961, e-mail: mv.caruso@unicz.it

Received: April 29th, 2015

Accepted for publication: September 21st, 2015

Abstract

Purpose: The extra-corporeal membrane oxygenation (ECMO) is a temporary, but prolonged circulatory support for cardiopulmonary failure. Clinical evidence suggests that pulsed flow is healthier than non pulsatile perfusion. The aim of this study was to computationally evaluate the effects of total and partial ECMO assistance and pulsed flow on hemodynamics in a patient-specific aorta model.

Methods: The pulsatility was obtained by means of the intra-aortic balloon pump (IABP), and two different cases were investigated, considering a cardiac output (CO) of 5 L/min: Case A - Total Assistance - the whole flow delivered through the ECMO arterial cannula; Case B - Partial assistance - flow delivered half through the cannula and half through the aorta.

Computational fluid dynamic (CFD) analysis was carried out using the multiscale approach to couple the 3D aorta model with the lumped parameter model (resistance boundary condition).

Results: In case A pulsatility followed the balloon radius change, while in case B it was mostly influenced by the cardiac one. Furthermore, during total assistance, a blood stagnation occurred in the ascending aorta; in case of partial assistance, the flow was orderly when the IABP was on and was chaotic when the balloon was off. Moreover, the mean arterial pressure (MAP) was higher in case B. The wall shear stress was worse in ascending aorta in case A.

Conclusions: Partial support is hemodynamically advisable.

Keywords: Extracorporeal Membrane Oxygenation (ECMO), Intra-Aortic Balloon Pump (IABP), Computation Fluid Dynamic (CFD), Multiscale Model, Aorta

1. Introduction

Extra-corporeal membrane oxygenation (ECMO) is a common procedure of the extra-corporeal circulation (ECC) used for patients with cardio-respiratory failure when they do not respond to conventional therapy [18], [1]. It is also used as a prolonged but temporary post-operative support after cardiac surgery and after the weakness from cardiopulmonary bypass (CPB) [21]. The main clinical complications of ECMO treatment are cerebral injuries and heart attacks [7], [20]. Moreover, other clinical problems, such as hemolysis, thromboembolic events and internal blending, can developed, which are related to interactions with the mechanical components and to the wall shear stress [9].

Generally, the flow during ECC is constant/ linear [2], as opposed to physiological perfusion, that has an important pulsatility. Several benefits can be obtained by using pulsed flow, such as the increase of brain perfusion and the reduction of the systemic inflammatory response syndrome (SIRS) [10]. Intra-Aortic Balloon Pump (IABP) was proposed as a useful device to provide pulsatile flow during CPB [3]. Its main component is a bio-compatible, elastic and resistant polyethylene balloon, placed in the descending aorta, that inflates and deflates or according to the cardiac cycle, using the electrocardiogram (ECG) signal [11], or setting the assistance level when there is no heart activity (no ECG signal), as in case of ECC. From a mechanical point of view, it is a volume displacement pump. Furthermore, it was demonstrated that IABP-induced pulsatile flow during extracorporeal circulation improves creatinine clearance and splanchnic enzymatic release [14], preserves lung functions in patients with chronic obstructive pulmonary disease (COPD) [13] and renal functions in patients undergoing myocardial revascularization [16], increases the hemocoagulative and fibrinolytic response [15] and the diastolic and mean blood flow, with a reduction in afterload [17].

The aim of this study was to evaluate the effects of pulsed induced-IABP flow during total and partial ECMO support on hemodynamics in a patient-specific aorta model. To carry out the analysis, the computational fluid dynamic (CFD) approach was chosen because it represents a valid, practical and efficient tool that allows to evaluate and investigate, in time and space, the two main fluid-dynamic parameters -the velocity and the pressure- through the resolution of numerical simulations [22].

2. MATERIALS AND METHODS

2.1 Geometrical model

Aorta geometry was reconstructed starting from a series of slices of a health aorta in a 54-year-old man, which were acquired *in-vivo* through the computer tomography (CT). This patient-specific aorta morphology was obtained using Itk-Snap 3.0, an open source segmentation software (www.itksnap.org/). Since it provides a stereolithographic file (stl format), the 3D aorta with faceted surfaces was converted in a 3D solid model by means of the reverse engineering process. The aorta model included the ascending aorta, the aortic arch with its three epiaortic vessels (brachiocephalic artery, left carotid artery, left subclavian artery) and the descending aorta.

To reproduce the perfusion during ECMO and the veno-arterial configuration, a standard arterial cannula (24 Fr Medtronic Inc., Minneapolis, MN, USA) was reconstructed and placed in the ascending aorta as in the clinical practice of our institution: 2 cm below the take off of the brachiocephalic artery on the anterior wall of the vessel, with a tilt angle of 45° respect to the transversal plane (Fig. 1).

As previously reported, pulsed flow during the extracorporeal circulation is better than the linear one. Therefore, a pulsatile perfusion was considered and obtained by means of the intra-aortic balloon (IABP). A balloon of 40 cm^3 was modeled (Sensation 7 Fr 40 cm^3 and CS300 IABP System, Datascope, Maquet GmbH and Co. KG, Rastatt, Germany). Furthermore, for simplicity, conical terminal parts were ignored. The complete geometrical 3D model used in this study is illustrated in Fig. 1.

2.2 Mathematical model

From a macroscopic point of view, the blood has a density of 1,060 Kg/m^3 and a non Newtonian behavior [5]. For large vessels as the aorta, it can be modeled as an incompressible and Newtonian fluid [8], with a viscosity of 0.0035 Pa·s [25]. Furthermore, its motion is described by the 3D Navier-Stokes equations:

$$\nabla \cdot u=0 \quad (1)$$

$$\rho\,(\partial u/\partial t)+\rho(u\cdot\nabla)u=\nabla\cdot[-pI+\mu(\nabla u+(\nabla u)T]+F \quad (2)$$

where u represents the fluid velocity vector, p the pressure, μ dynamic viscosity, ρ the density of the blood, I the identity matrix and F the volume force field. The last variable was neglected in this computational analysis because, during the surgical procedure, the patient was supine, so there is no gravity effect.

Because during the partial ECMO assistance half of the inlet flow is provided by the heart, the inflation of the balloon was synchronized to the cardiac cycle: it was fully deflated in systolic peak and it was fully inflated in middle diastole. Its inflation/deflation behavior was numerically reproduced by means of a parametric study in which the radius changed according an 8 degree Fourier equation during the cardiac cycle (Fig. 2).

2.3 Boundary conditions

To compare the total support with the partial one, a cardiac output (CO) of 5 L/min was considered and two different inlet boundary conditions were applied:

- Case A- total ECMO assistance: the whole flow was delivered by ECMO circuit through the arterial cannula, with a fully developed profile; in this case the aorta was considered as clumped;
- Case B- partial ECMO assistance: the flow was delivered through the arterial cannula (fully developed profile with a value of 2.5 L/min) and from the heart (fully developed profile with a value of 2.5 L/min and physiological pulsatility) – Fig. 2.

Because we did not have clinical pressure or flow data during partial and total ECMO support with the IABP, in our study we implemented a multiscale model 3D-0D [19] in order to specify the outlet boundary conditions. To specify the relationship between flow and pressure, resistance conditions were adopted, as in other studies [4], [6], [23], [24]. Resistances at the four outflow exits (brachiocephalic artery, left common carotid artery, left subclavian artery and thoracic aorta) were imposed by the following equation:

$$p=p_0+R\cdot Q \qquad (3)$$

where p_0 is an outlet pressure offset, Q indicates the instantaneous volumetric flow rate through each respective outflow exit, calculated at each instant from the local velocity profile, and R the resistance. R values were evaluated in order to specify the flow rate in respect to the inlet flow of about 16% in the brachiocephalic artery, 8% in left carotid and left subclavian arteries and the remain percentage in the descending aorta, as in physiological situation. These values were used both in case of total and partial support of ECMO and IABP hypothesizing that the blood demand depends on the needs of organs and tissues and so that the percentages flow rate is the same in the two type of support. Furthermore, p_0 was calculated to ensure the mean arterial pressure (MAP) maintained during ECMO support (MAP>70mmHg) [7].

Moreover, because we did not have clinical data regarding the wall elasticity during ECMO and IABP in case of total and partial support and because the main task of our work is the

comparison between hemodynamics in case of partial and total support during ECMO and IABP, we hypothesized the vessels as rigid and the no-slip boundary conditions were applied, approximation adopted in other studies [4], [6], [24], and we derived the conclusions on the basis of rigid wall model. Furthermore, rigid wall assumption is also frequently adopted to reduce computational cost, as required in case of FSI, and to obtain a preliminary study for evaluating the hemodynamics. Moreover, also the arterial cannula was considered as a rigid domain.

2.4 Simulation details

Computational analysis was carried out using COMSOL 5.0 (COMSOL Inc, Stockholm, Sweden), a finite-element-based commercial software package. A mesh with 394,850 tetrahedral elements was created considering a minimum element quality of 0.1154 and an element volume ratio of $6.641 \cdot 10^{-5}$. Furthermore, the percentage error related to the grid was evaluated as:

$$e = | (CO - CTF)/CO| \cdot 100 \quad (4)$$

where CO is the cardiac output considered and imposed as an inlet boundary condition and CTF is the calculated total flow, expressed as:

$$CTF = \sum q_i \quad (5)$$

with i=0-4 and indicating the branch (Table 1). The mesh used in the study generated an error less than 5% both in case A and in case B, an acceptable error to consider the solution grid independent.

Two parametric simulations were computed, considering a cardiac cycle of 1 s and a step of 0.001. In both cases, fluid dynamic laws were approximated with a first order difference scheme (P1-P1). Furthermore, the convergence criteria were set at 10^{-4}. Four cardiac cycles were simulated in order to eliminate the transitory effects due to the convergence process. The last cycle (3-4 s) was considered to analyze hemodynamics.

3. Results

The flow waveforms for each vessel and for the arterial cannula, evaluated in one cardiac cycle (3-4 *s*), are reported in Fig. 3, which considers the total support and the partial one. Different waveforms occur: in case A flows follow the balloon radius change behavior, with the same trend for the epiaortic vessel and on opposite trend for the descending aorta; in case

B flows follow the ventricular flow and a small diastolic augmentation appear in the epiaortic vessels. Moreover, considering the epiaortic vessels, in case A the maximum flow is twice greater than the one in case B, whereas the minimum is about the half value obtained in case B (Table 2). The pulsatility of flow can be evaluated as the difference between the maximum value (systolic peak) and the minimum one (diastole). This value is reported in Table 2 and it is low in case A and high in case B.

In Fig. 4 the stream lines of the velocity magnitude are shown, considering the systolic peak (IABP-off, 1) and the middle diastole (IABP-on, 2). During total assistance (A1-A2) the ascending aorta is characterized by big vortexes in both instants, so blood stasis occurs. Furthermore, the epiaortic vessels present whirling flow. In case of partial assistance (B), when the IABP is closed (B1), the flow is orderly, both in aorta and in the epiaortic vessels. However, when the IABP obstructed the descending aorta (B2), the flow in ascending aorta is orderly but with low value, two vortexes are generated near the cannula anastomosis and the flow has a chaotic profile in the epiaortic vessels.

The pressure trends over one cardiac cycle are presented in Fig. 5. Since resistances are adopted as outlet boundary conditions, also pressure behavior follows the IABP radius change variation as the flow. Therefore the pulsatility amplitude of pressure is lower in case of total support (A) than in case of partial assistance (B). Furthermore, the mean arterial pressure MAP is about 74.3±3.8 mmHg in case of flow delivered only by means of ECMO and about 81.7±2.0 mmHg in case of flow delivered both by the extra-corporeal circulation and the heart.

In addition to the two fluid-dynamic variables, the viscous stress generated by the flow was analyzed. The wall shear stress (WSS) pattern is illustrated in Fig. 6. In case A the WSS is always low in the ascending aorta and in the aortic arch, except for the emergence of the epiaortic vessels, in which it is about 2 Pa, both in case of IABP-on and IABP-off. Moreover, a WSS of about 1.5 Pa occurs in the wall opposite the cannula anastomosis. In case of partial support (B), in systolic peak the most stressed areas are the emergence of left subclavian and left carotid arteries (about 5 Pa), while in the diastolic instant the WSS is lower (about 1.5 Pa). Moreover, as in case of total assistance, also during partial support when the IABP is on the WSS is low in ascending aorta and in the aortic arch.

4. Discussion

The correct modality of perfusion in terms of pulsatile or non-pulsatile flow during extra-corporeal circulation and the relative effects on hemodynamics were extensively investigated

[10]. Typically, veno-arterial ECC is run at about 80% of resting cardiac output in order to maintain an arterial pulse contour [2]. In this work, hemodynamics in the aorta during total perfusion and partial perfusion in ECMO circulation considering the IABP-induced pulsed flow was evaluated and analyzed by means of the computational approach, deriving the conclusion on the basis of rigid wall assumption.

To specify the outlet boundary conditions, a multi-scale model 3D-0D [19] was implemented coupling the lumped parameter model with the 3D one, using the resistance condition for specifying the relationship between flow and pressure. Moreover, this condition allowed to clarify the percentage of flow rate [4], [24]. In this study it was hypothesized that resistance values remain the same in both total (case A) and partial support (case B), because blood demand depends on the needs of organs and tissues. So, it was considered that the flow rate percentage is independent from the perfusion modality. For this reason, our study compared the flow and pressure distribution and the velocity pattern considering the difference in the inlet boundary condition of perfusion (only ECMO or ECMO and aorta). So, for each vessel the mean flow is approximately the same both in case A and in case B (Table 3), although different waveforms occur (Fig. 3). Moreover, in case A the descending aorta presents an opposite trend in respect to the other vessels due to the occlusion of the lumen when the IABP is on (diastolic instant). On the contrary, in case of partial support (case B) flow pulsatility is strongly influenced by heart activity and a small diastolic augmentation appears in epiaortic vessels. Furthermore, the flow in the descending aorta decreases but not beyond the minimum one (about 2 L/min) as in case A (from 3.74 L/min to about 3 L/min).

Regarding the velocity pattern, the ascending aorta is characterized by blood stagnation during total support, both with IABP-on and IABP-off, whereas in case of double perfusion (partial support with ECMO) the flow is always orderly.

Atherosclerotic events are correlated to the wall shear stress, whose good level is of about 1.5-2.0 Pa [12]. In the locations with blood flow recirculation and stasis, WSS is low, of about 0.4 Pa, so an high probability of atherosclerotic plaque formation occurs [12]. Low WSS is recorded in the ascending aorta (Fig. 6), but only in case of total support the flow is chaotic (Fig. 4). This means that in this case (A) atherogenesis involves the walls of this trunk.

Regarding pressure, the CFD model was implemented ensuring a MAP>70 mmHg as in clinical practice and the numerical results confirmed these conditions. Moreover, MAP is higher in partial support than in total one. A particular situation occurs in case of total support in the descending aorta, that does not present a positive pulsatility like in physiological case

because the resistance condition was used as outlet boundary condition. As a consequence, its trend is the same as the flow waveform.

5. Conclusion

This computational analysis has highlighted that, although IABP can be used to provide a flow pulsatility, the pulse contour is higher and more similar to the physiological one when there is a percentage of blood flow provided by the heart. Furthermore, several velocity patterns and consequently wall shear stresses were recorded, suggesting that partial perfusion is more advisable.

Although this CFD study provides more information regarding the hemodynamics during ECMO and IABP support, it has some limitations, as the rigid wall approximation. So, a future perspective is considering the contribution of wall on hemodynamics implementing a fluid-structure interaction (FSI) and using the results obtained from ex-vivo experimental tensile tests on aortic tissue as data of structural mechanical behavior and of wall deformation laws. Moreover, in order to obtain realistic changes in the mean blood flow values, we will applied in-vivo clinical data as outlet boundary conditions in the computational model.

References

[1]. Anderson III H.M.D., Chapman R., Hirschl R., Bartlett, R. Extracorporeal life support for adult cardiorespiratory failure, Surgery, 1993, vol. 114(2), 161-172.

[2]. Bartlett R.H. Extracorporeal life support for cardiopulmonary failure, Curr Probl Surg, 1990, vol. 27(10), 627-705.

[3]. Bregman D., Bowman Jr. F.O., Parodi E.N., Haubert S.M., Edie R.N., Spotnitz H.M., Malm J.R. An improved method of myocardial protection with pulsation during cardiopulmonary bypass, Circulation, 1977, vol. 56(3), II157-60.

[4]. Caruso M.V., Gramigna V., Rossi M., Serraino G.F., Renzulli A., Fragomeni G. A computational fluid dynamics comparison between different outflow graft anastomosis locations of Left Ventricular Assist Device (LVAD) in a patient- specific aortic model, Int J Numer Method Biomed Eng, 2015, vol. 31(2), 1-12.

[5]. Cutnell J.D., Johnson, K.W. Physics, Wiley, 1998.

[6]. De Zelicourt D., Jung P., Horner M., Pekkan K., Kanter K. R., Yoganathan A.P. Cannulation strategy for aortic arch reconstruction using deep hypothermic circulatory arrest, Ann Thorac Surg, 2012, vol. 94(2), 614-620.

[7]. Doll N., Kiaii B., Borger M., Bucerius J., Krämer K., Schmitt D. V., Mohr, F.W., Five-year results of 219 consecutive patients treated with extracorporeal membrane oxygenation for refractory postoperative cardiogenic shock, Ann Thorac Surg, 2004, vol. 77(1), 151-157.

[8]. Formaggia L., Quarteroni A.M., Veneziani A. Cardiovascular mathematics (No. CMCS-BOOK-2009-001), Springer, 2009.

[9]. Goubergrits L., Numerical modeling of blood damage: current status, challenges and future prospects, Expert Rev Med Devices, 2006, vol. 3(5), 527-531.

[10]. Ji B., Ündar A. An evaluation of the benefits of pulsatile versus nonpulsatile perfusion during cardiopulmonary bypass procedures in pediatric and adult cardiac patients, ASAIO Journal, 2006, vol. 52(4), 357-361.

[11]. Krishna M., Zacharowski K. Principles of intra-aortic balloon pump counterpulsation, Continuing Education in Anaesthesia, Critical Care & Pain, 2009, vol. 9(1), 24-28.

[12]. Malek A.M., Alper S.L., Izumo, S. Hemodynamic shear stress and its role in atherosclerosis, Jama, 1999, vol. 282(21), 2035-2042.

[13]. Onorati F., Cristodoro L., Bilotta M., Impiombato B., Pezzo F., Mastroroberto,P., Renzulli A. Intraaortic balloon pumping during cardioplegic arrest preserves lung

function in patients with chronic obstructive pulmonary disease, Ann Thorac Surg, 2006, vol .82(1), 35-43.

[14]. Onorati F., Cristodoro L., Mastroroberto P., di Virgilio A., Esposito A., Bilotta M., Renzulli A. Should we discontinue intraaortic balloon during cardioplegic arrest? Splanchnic function results of a prospective randomized trial, Ann Thorac Surg, 2005, vol. 80(6), 2221-2228.

[15]. Onorati F., Esposito A., Comi M. C., Impiombato B., Cristodoro L., Mastroroberto P., Renzulli A. Intra-aortic balloon pump-induced pulsatile flow reduces coagulative and fibrinolytic response to cardiopulmonary bypass, Artif Organs, 2008, vol. 32(6), 433-441.

[16]. Onorati F., Presta P., Fuiano G., Mastroroberto P., Comi N., Pezzo F., Renzulli A. A randomized trial of pulsatile perfusion using an intra-aortic balloon pump versus nonpulsatile perfusion on short-term changes in kidney function during cardiopulmonary bypass during myocardial reperfusion. Am J Kidney Dis, 2007, vol. 50(2), 229-238.

[17]. Onorati F., Santarpino G., Rubino A., Cristodoro L., Scalas C., Renzulli A., Intraoperative bypass graft flow in intra-aortic balloon pump–supported patients: Differences in arterial and venous sequential conduits, J Thorac Cardiovasc Surg, 2009, 138(1):54-61.

[18]. Paolini G., Triggiani M., Di Credico G., Pocar M., Stefano P., Montorsi E., Grossi A. Assisted Circulation in Pericardiotomy Heart Failure: Experience with the Bio-Medicus Centrifugal Pump in ten Patients. Vascular, 1994, vol. 2(5), 630-633.

[19]. Quarteroni A., Veneziani A. Analysis of a geometrical multiscale model based on the coupling of ODE and PDE for blood flow simulations, Multiscale Modeling & Simulation, 2003, vol. 1(2), 173-195.

[20]. Risnes I., Wagner K., Nome T., Sundet K., Jensen J., Hynås I.A., Svennevig J.L. Cerebral outcome in adult patients treated with extracorporeal membrane oxygenation, Ann Thorac Surg, 2006, vol. 81(4), 1401-1406.

[21]. Smith C., Bellomo R., Raman J.S., Matalanis G., Rosalion A., Buckmaster,ì J., Buxton B.F. An extracorporeal membrane oxygenation–based approach to cardiogenic shock in an older population, Ann Thorac Surg, 2001, vol. 71(5), 1421-1427.

[22]. Tu J., Yeoh G.H., Liu, C. Computational fluid dynamics: a practical approach, Butterworth-Heinemann, 2007.

[23]. Vignon-Clementel I.E., Marsden A.L., Feinstein J.A. A primer on computational simulation in congenital heart disease for the clinician. Prog Pediatr Cardiol, 2010, vol. 30(1), 3-13.

[24]. Yang N., Deutsch S., Paterson E.G., Manning, K.B. Comparative study of continuous and pulsatile left ventricular assist devices on hemodynamics of a pediatric end-to-side anastomotic graft, Cardiovasc Eng Technol, 2010, vol. 1(1), 88-103.

[25]. Yilmaz F., Gundogdu M.Y. A critical review on blood flow in large arteries; relevance to blood rheology, viscosity models, and physiologic conditions, Korea-Australia Rheology Journal, 2008, vol. 20(4), 197-211.

Figures:

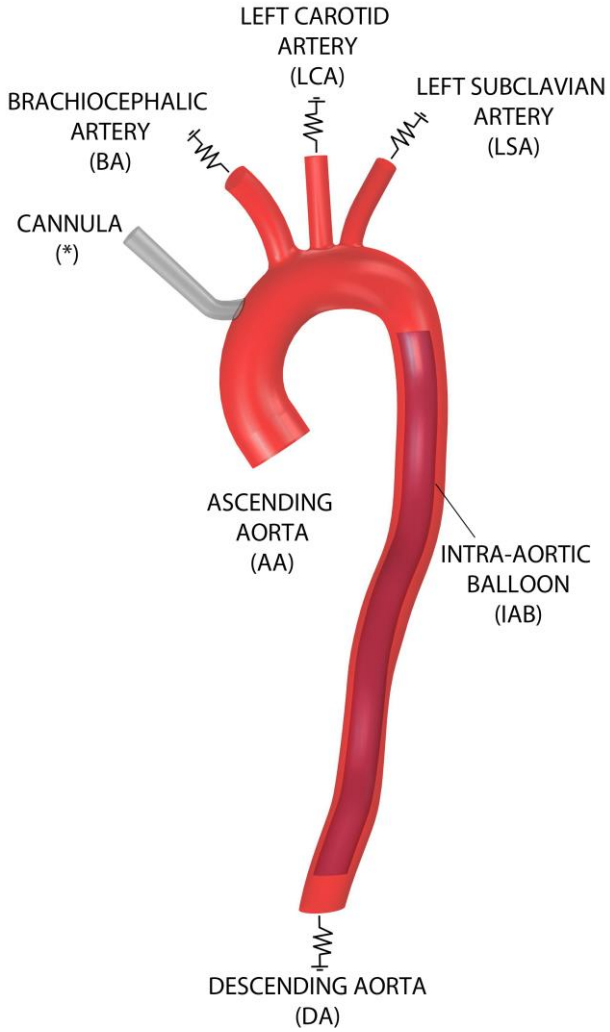

Figure 1: Multi-scale model: 3D patient-specific aorta model and lumped parameter model (resistance boundary condition). Note: in round brackets abbreviations are specified.

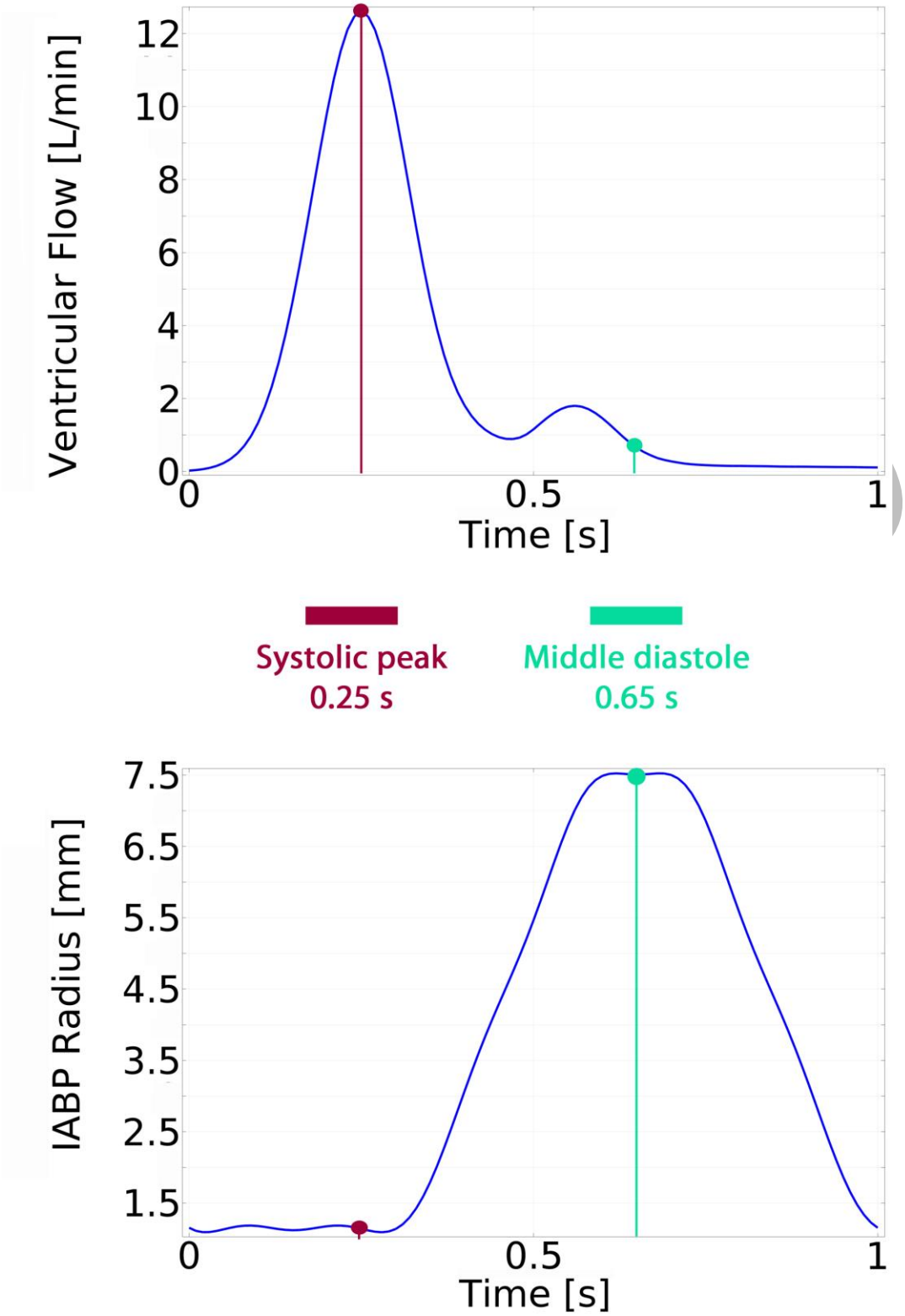

Figure 2: Ventricular flow (up) with a mean cardiac output of 2.5 L/min and the IABP radius change behavior (down). Note: IABP-off in systolic peak, IABP-on in middle diastole.

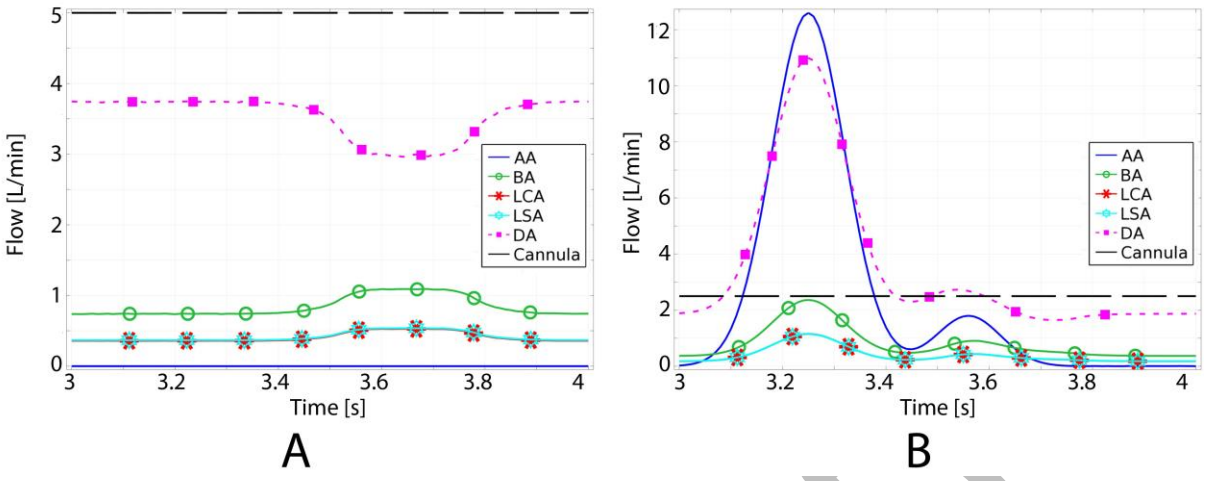

Figure 3: Flow waveforms in the ascending aorta (AA), in the epiaortic vessels (BA, LCA and LSA), in the descending aorta (DA) and in the arterial cannula in case of total support (A) and partial one (B) during one cardiac cycle.

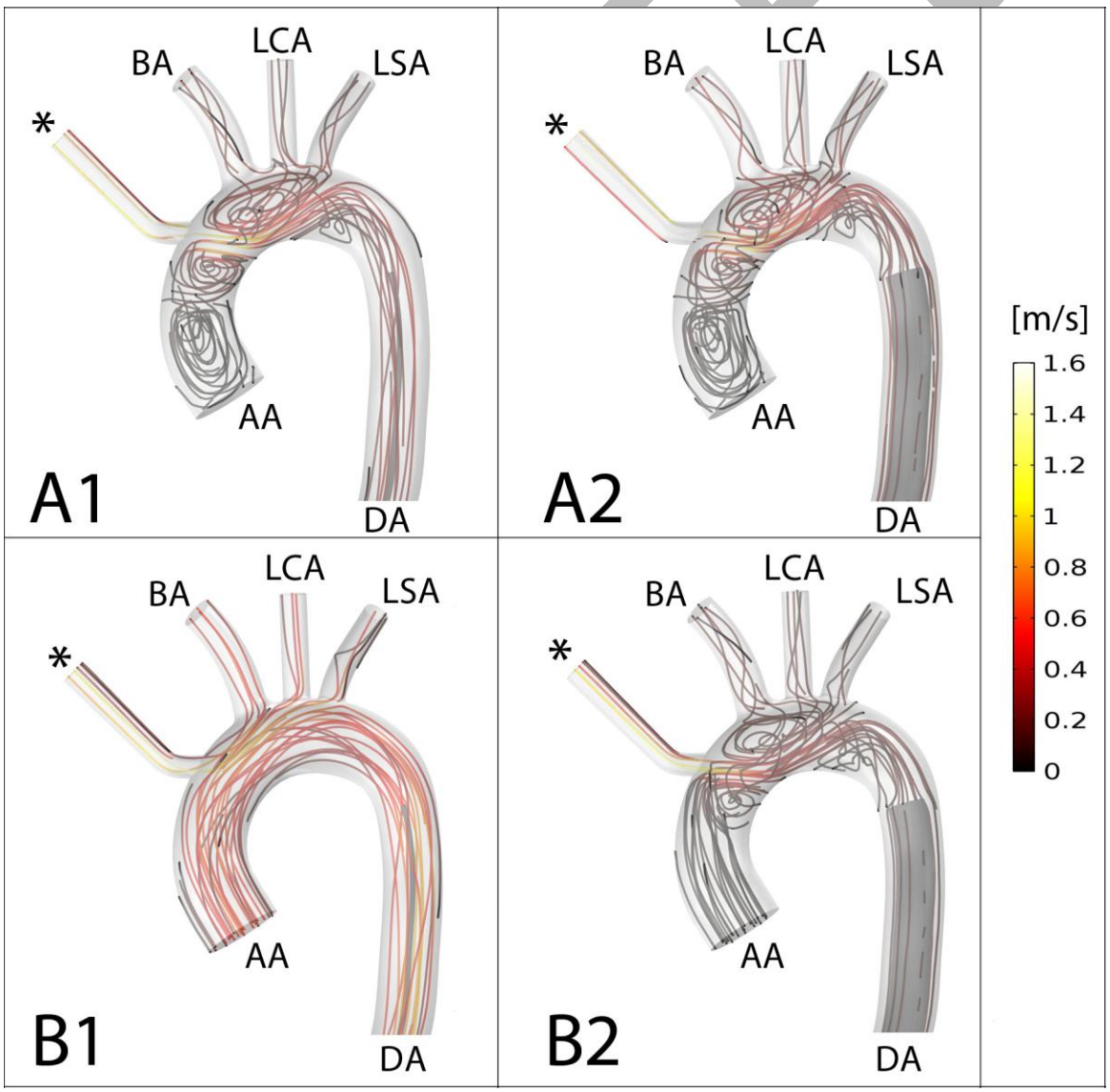

Figure 4: Volume stream lines of velocity magnitude in the ascending aorta (AA), in the epiaortic vessels (BA, LCA and LSA), in the descending aorta (DA) and in the arterial cannula in case of total support (A) and partial one (B) considering the systolic peak (1) and the middle diastole (2).

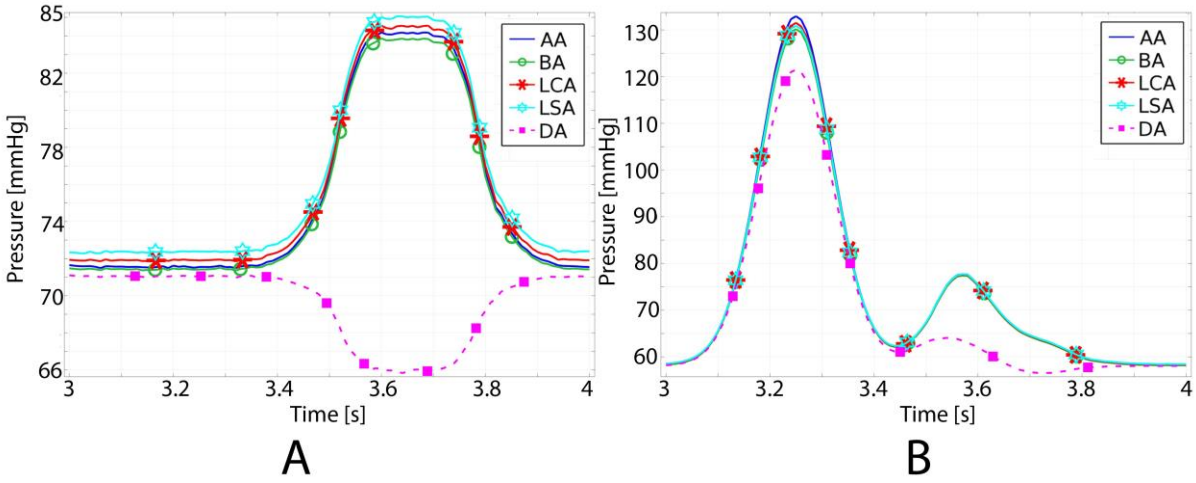

Figure 5: Pressure waveforms in ascending the aorta (AA), in the epiaortic vessels (BA, LCA and LSA), in the descending aorta (DA) and in the arterial cannula in case of total support (A) and partial one (B) during one cardiac cycle.

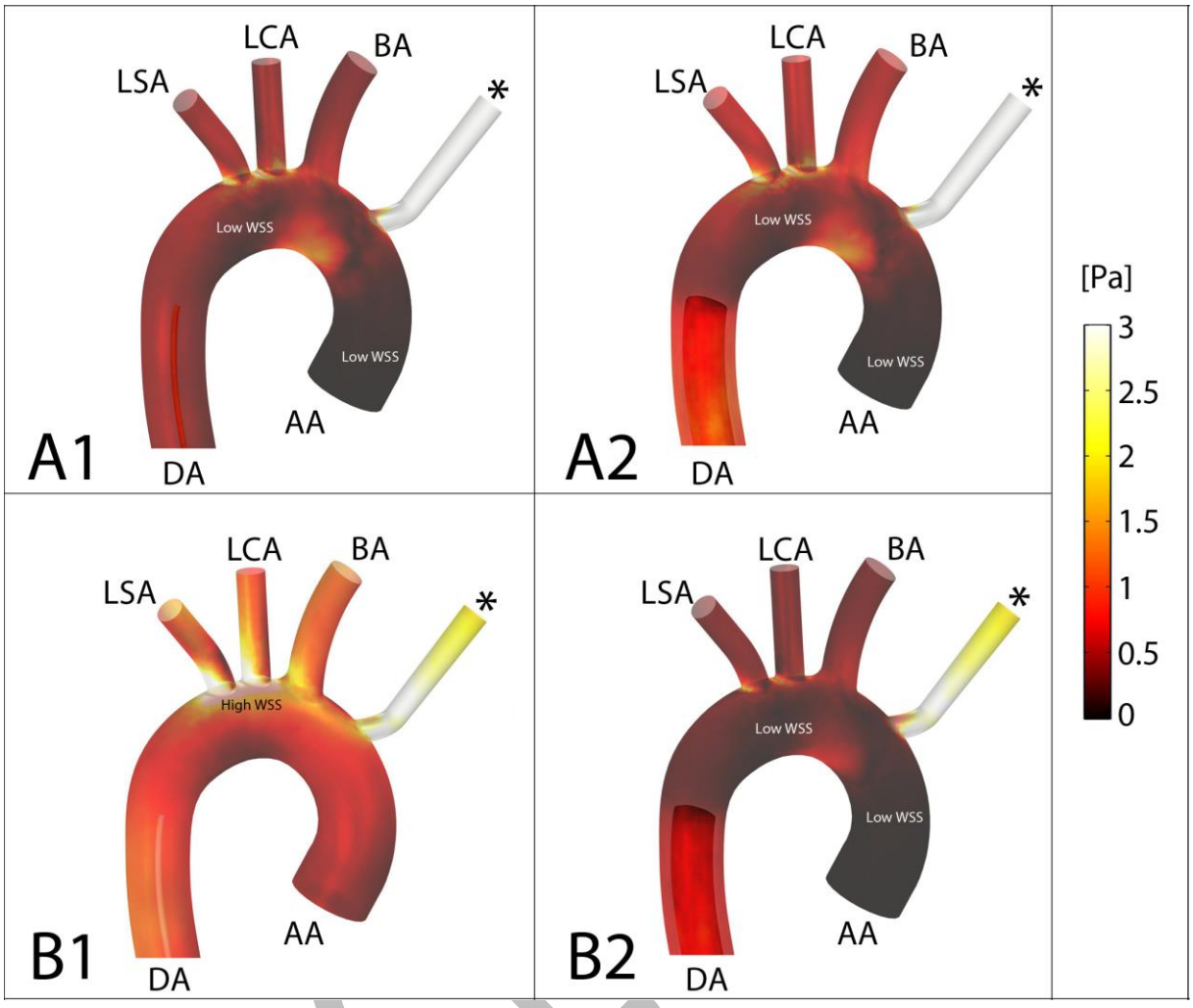

Figure 6: Wall shear stress pattern in the ascending aorta (AA), in the epiaortic vessels (BA, LCA and LSA), in the descending aorta (DA) and in the arterial cannula in case of total support (A) and partial one (B) considering the systolic peak (1) and the middle diastole (2).

Tables:

Table 1: Mean flow during total (case A) and partial (case B) assistance in each vessel and in the cannula. The percentage error is also reported. CTF: computational total flow.

i	Branch	CASE A	CASE B
		Mean flow [L/min]	
0	AA	0.00	2.49
1	BA	0.84	0.81
2	LCA	0.41	0.39
3	LSA	0.42	0.39
4	DA	3.53	3.59
5	Cannula	5.00	2.50
CTF		5.20	5.18
e [%]		3.95	3.66

Table 2: Flow in each epiaortic vessel and in arterial cannula in total ECMO perfusion (case A) and partial one (case B) in systolic peak (SP) and in diastole (D). The amplitude of pulsatility, evaluated as SP- D, is also reported.

Vessel		BA	LCA	LSA
CASE A	Systolic peak (SP) [L/min]	1.09	0.53	0.54
	Diastole (D) [L/min]	0.74	0.36	0.37
	Pulsatility Amplitude (SP - D) [L/min]	0.35	0.17	0.17
CASE B	Systolic peak (SP) [L/min]	2.36	1.15	1.15
	Diastole (D) [L/min]	0.37	0.18	0.18
	Pulsatility Amplitude (SP - D) [L/min]	1.99	0.97	0.97